

Technology Reports

LTE-Advanced—Evolution of LTE— Radio Transmission Experiments

The expanded use of smartphones and tablet computers in recent years has brought about a dramatic increase in data traffic in the radio access network, which is expected to grow to even higher levels in the years to come. To meet this demand for radio access, the standardization of LTE-Advanced—an evolution of LTE—is now in progress. This article describes experimental equipment constructed for testing the radio access technology adopted by LTE-Advanced and presents the results of field and indoor experiments on these LTE-Advanced radio access technologies using an LTE-Advanced transceiver.

Radio Access Network Development Department

Teruo Kawamura**Yoshihisa Kishiyama****Yuichi Kakishima****Shinpei Yasukawa****Keisuke Saito****Hidekazu Taoka**DOCOMO Communication Laboratories
Europe GmbH

1. Introduction

Launched in December 2010, NTT DOCOMO's "Xi" (Crossy) is a mobile communications service conforming to the LTE standard [1]. It achieves higher data rates, higher capacities and lower latencies than FOMA. LTE (whose initial release corresponds to Release 8 specifications) adopts a variety of radio access technologies such as intra-cell orthogonal multiple access schemes (downlink: Orthogonal Frequency Division Multiple Access (OFDMA)^{*1}; uplink: Single

Carrier-Frequency Division Multiple Access (SC-FDMA)^{*2}), frequency domain scheduling^{*3} and Multiple-Input Multiple-Output (MIMO)^{*4} transmission in the downlink [2].

Against this background, the spread of data-intensive services such as video delivery is expected to increase data traffic even further in the years to come. To meet this growing demand for radio access in a timely manner, NTT DOCOMO looks to make further improvements in system performance in the radio access network and is promoting the standardization of LTE-

Advanced, an evolution of LTE. The LTE standard has been continuously updated since Release 8, and LTE-Advanced corresponds to LTE Release 10 and beyond [3]. Standardization of Release 10 specifications for the LTE-Advanced radio interface has already been completed and standardization activities for Release 11 are now underway. LTE-Advanced must maintain backward compatibility with LTE (Release 8/9) and must satisfy the requirements of International Mobile Telecommunication (IMT)-Advanced [4]. LTE-Advanced has therefore

©2012 NTT DOCOMO, INC.

Copies of articles may be reproduced only for personal, noncommercial use, provided that the name NTT DOCOMO Technical Journal, the name(s) of the author(s), the title and date of the article appear in the copies.

*1 **OFDMA**: A multiple access scheme that uses Orthogonal Frequency Division Multiplexing (OFDM). OFDM uses multiple low data rate multi-carrier signals for the parallel transmission of wideband data with a high data rate, thereby implementing high-quality transmission that is highly robust to multipath interference (interference from delayed paths).

adopted Carrier Aggregation (CA)^{*5} to achieve wider transmission bandwidths up to 100 MHz [5]. It has also adopted advanced multi-antenna technologies including MIMO transmission in the uplink, extensions of MIMO transmission in the downlink (such as Multi-User (MU)-MIMO^{*6}) and Coordinated Multi-Point (CoMP) transmission/reception^{*7} [6][7].

The authors have constructed LTE-Advanced real-time radio-transmission experimental equipment based on Release 10 specifications and have so far performed experimental evaluations of radio access technologies in LTE-Advanced [8]-[15]. In this article, we describe the experimental equipment that we have constructed and present the results of field and indoor experiments on these LTE-Advanced radio access technologies using an LTE-Advanced transceiver.

2. Implementation on Experimental Equipment

The experimental equipment that we constructed for evaluating LTE-Advanced radio access technology supports asymmetric CA (downlink: 100 MHz; uplink 40 MHz), which means wider transmission bandwidth achieved by using contiguous bands and different transmission bandwidths in the downlink and uplink in the Frequency Divi-

sion Duplex (FDD)^{*8} scheme. This equipment also supports advanced multi-antenna technologies such as 2 × 2 Single User (SU)-MIMO (spatial multiplexing and closed-loop transmit diversity^{*9} with precoding) in the uplink, 4 × 2 MU-MIMO in the downlink, and CoMP transmission in the downlink using Remote Radio Equipment (RRE) with an optical-fiber connection.

2.1 CA

The basic concept of CA in LTE-Advanced is shown in **Figure 1**. CA is a technology that achieves wider transmission bandwidths while maintaining compatibility with LTE (Release 8/9). It treats the frequency block (or Component Carrier (CC)) having a maximum bandwidth of 20 MHz as a basic unit of connection with an LTE terminal and supports expanded bandwidths up to 100 MHz using 5 CCs. LTE-Advanced supports not only CA using

contiguous CCs but also CA using non-contiguous CCs as well as asymmetric CA that allocates a different number of CCs to the downlink and uplink in the FDD scheme [16][17]. These schemes make for flexible spectrum allocation. Asymmetric CA can be used, for example, in packet-type services in which traffic is quite heavy in the downlink (as when downloading Web content) compared to that in the uplink. The experimental equipment introduced here implements asymmetric CA using contiguous CCs.

LTE-Advanced performs Adaptive Modulation and Coding (AMC)^{*10} and Hybrid Automatic Repeat reQuest (HARQ)^{*11} for each transmission stream of each CC as well as in LTE. To provide flexible support for AMC and HARQ in the downlink in asymmetric CA, the MS transmits Uplink Control Information (UCI) such as Channel Quality Indicator (CQI)^{*12} and Acknowledgement (ACK)/Negative

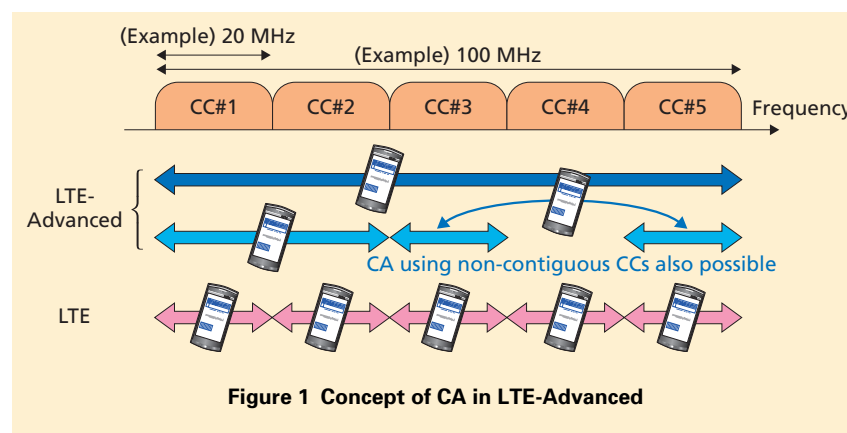


Figure 1 Concept of CA in LTE-Advanced

*2 **SC-FDMA**: A multiple access scheme that employs single carrier transmission for an individual user and achieves multiple access by allocating the signals for different users to different frequencies.

*3 **Frequency domain scheduling**: A technology for scheduling radio resources allocated to each user and obtaining a diversity effect between users by using fluctuation on the propagation channel in the frequency domain.

*4 **MIMO**: A signal transmission technology that improves communications quality and spectral efficiency by using multiple transmitter and receiver antennas for transmitting signals at the same time and same frequency.

*5 **CA**: A technology that achieves high-speed communications through bandwidth expansion while maintaining backward compatibility with existing LTE by performing simultaneous transmission and reception using multiple component carriers.

*6 **MU-MIMO**: A technology that improves spectral efficiency by applying MIMO multiplexed transmission to the signals for multiple users.

*7 **CoMP transmission/reception**: A technology that transmits or receives signals from multiple sectors or cells to and from a given UE. By coordinating transmission/reception among multiple cells, interference from other cells can be reduced and the power of the desired signal can be increased.

ACK (NACK) from one predetermined CC. In this way, UCI can be transmitted without increasing the Peak-to-Average Power Ratio (PAPR)^{*13} in an uplink based on SC-FDMA. In this experimental equipment, UCI for all downlink transmission streams and all CCs is encoded all together and mapped to the Physical Uplink Shared Channel (PUSCH) for transmission.

2.2 Uplink SU-MIMO

LTE-Advanced aims for a high peak spectral efficiency of 15 bit/s/Hz in the uplink, and to achieve this, it supports MIMO spatial multiplexing having a maximum of four transmission streams. It also supports closed-loop transmit diversity using multiple transmitter antennas. In transmit diversity, a scheme with precoding based on a codebook^{*14} is adopted, and to maintain a low PAPR, wideband precoding using a common precoding weight over contiguously allocated Resource Blocks (RB)^{*15} is also adopted. The concept of uplink SU-MIMO is shown in **Figure 2**. Here, a Mobile Station (MS) periodically transmits a Sounding Reference Signal (SRS) to each transmitter antenna. The Base Station (BS) estimates the MIMO channel response using the received SRS and performs adaptive radio link control (i.e., determines rank number, precoding weight, and the Modulation and Coding Scheme

(MCS)^{*16}). The MS then generates and transmits a data signal based on the parameters determined at the BS. In the evaluation, switching of rank number is performed semi-statically which doesn't aim to track instantaneous fading variations. Furthermore, rank 1 corresponds to the closed-loop transmit diversity with precoding and rank 2 to the MIMO spatial multiplexing in which each antenna transmits an independently encoded stream using a 2×2

antenna configuration.

The sub-frame configuration in the uplink for this experimental equipment is shown in **Figure 3**. To measure reception quality across the entire band, the SRS transmission bandwidth has been set to 96 RB (17.28 MHz) per CC regardless of the transmission bandwidth for the data signal. A sub-frame, which is 1 msec in length, consists of 14 SC-FDMA symbols^{*17}. Here, SRS is multiplexed on the last symbol (the

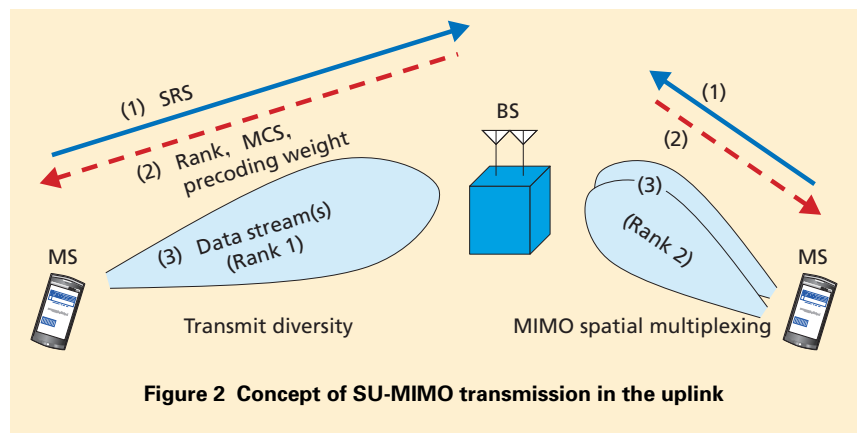


Figure 2 Concept of SU-MIMO transmission in the uplink

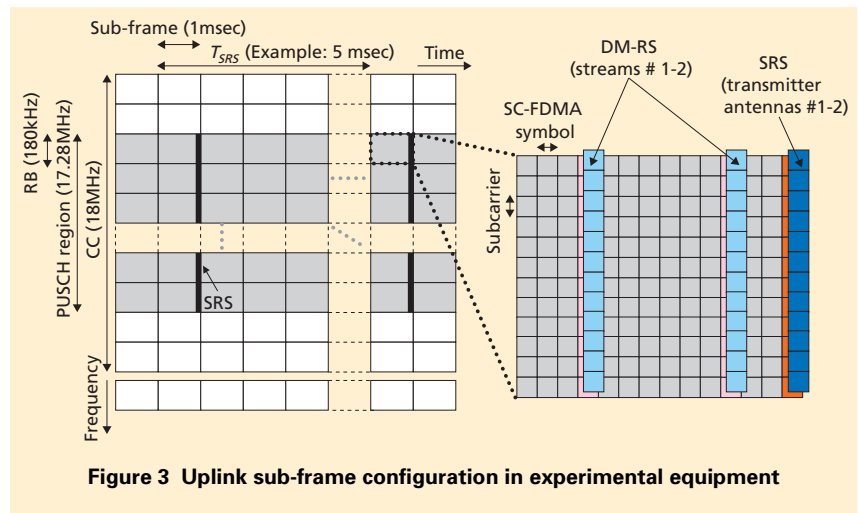


Figure 3 Uplink sub-frame configuration in experimental equipment

*8 **FDD**: A scheme for transmitting signals using different carrier frequencies and bands in the uplink and downlink.

*9 **Closed-loop transmit diversity**: A technology that obtains diversity gain and improves communications quality by using the difference in the fluctuation of propagation channels between transmitter antennas. A method within this technology that uses feedback from the receiver side.

*10 **AMC**: A method for adaptively controlling data rate by selecting the most appropriate MCS (see *16) according to the quality of received signals based, for example, on SINR.

*11 **HARQ**: A technology that combines Automatic Repeat request (ARQ) and error correcting codes to improve error-correcting ability on a retransmission and reduce the number of retransmissions. A packet retransmission method that improves reception quality and

achieves efficient transmission by combining resent data with previously received data.

*12 **CQI**: An index of reception quality measured at the mobile station expressing propagation conditions on the downlink.

14th symbol) and transmitted periodically at intervals corresponding to a T_{SRS} sub-frame. Code Division Multiplexing (CDM)^{*18} is applied to the multiplexing of SRS from each transmitter antenna through a cyclic shift of the same Reference Signal (RS) sequence. In addition, Demodulation RS (DM-RS), which is used in channel estimation^{*19} for data demodulation purposes, uses the same band as the data signal multiplexing at the 4th and 11th symbols of each sub-frame. When applying MIMO spatial multiplexing, CDM by cyclic shift is applied to the multiplexing of DM-RS for two streams as well as for SRS.

2.3 Downlink MU-MIMO

Downlink MU-MIMO has been specified as a required technology in LTE-Advanced to satisfy the spectral-efficiency requirements of IMT-Advanced [4]. This experimental equipment applies four BS transmitter antennas and two MS receiver antennas (maximum two transmission streams per MS)—the same as the evaluation requirements of IMT-Advanced—and evaluates MU-MIMO performance with 2 MSs. The target here is to achieve a total peak throughput of approximately 1 Gbit/s by transmitting a total of four streams simultaneously to these 2 MSs. The concept of MU-MIMO transmission in the downlink

for this experimental equipment is shown in **Figure 4**. Here, the BS periodically transmits Channel State Information (CSI)^{*20}-RS used for estimating CSI for each transmitter antenna at each MS, and each MS returns feedback to the BS on CSI estimated by using the received CSI-RS. Using this CSI feedback, the BS generates precoding weights to suppress mutual interference between the 2 MSs using beam forming. Then, for each data stream, the BS multiplexes the generated precoding weights on both the data signal and DM-RS, and finally transmits the signals.

When having a BS spatially multiplex and transmit more data streams than the number of MS receiver antennas as in the MU-MIMO configuration of this experimental equipment, highly accurate CSI feedback is needed to gen-

erate precoding weights for transmission (beam forming) to suppress mutual interference between the transmission streams of the 2 MSs. For this reason, we have implemented high-accuracy CSI feedback in the unit of sub-band for the experimental equipment as described below. This form of CSI feedback has not yet been specified in LTE-Advanced.

The sub-frame configuration in the downlink for this experimental equipment is shown in **Figure 5**. Each CC consists of multiple sub-bands, where a sub-band is the frequency unit for providing CSI feedback and applying common precoding weights. Sub-band size (F_{CSI}) is defined as a multiple number of RBs, where each RB consists of 12 sub-carriers^{*21} (180 kHz). In addition, a sub-frame, which is 1 msec in length, consists of 14 OFDM symbols. Here, CSI-

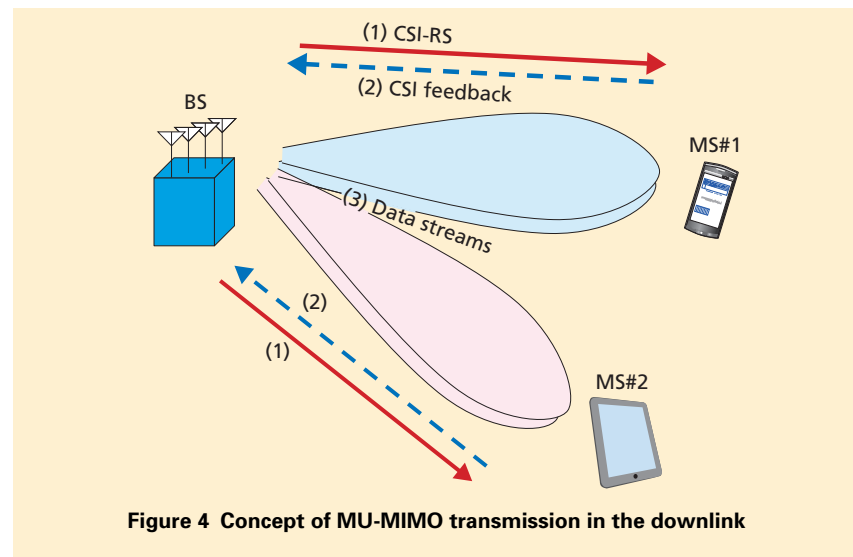


Figure 4 Concept of MU-MIMO transmission in the downlink

*13 **PAPR**: An index expressing the peak magnitude of the transmitted waveform defined as the ratio of maximum power to average power. If this value is large, the power amplifier back-off has to be made large to avoid signal distortion, which is particularly problematic for mobile terminals.

*14 **Codebook**: A set of predetermined precoding-weight matrix candidates.

*15 **RB**: The smallest unit of time or frequency

allocation when scheduling radio resources.

*16 **MCS**: A predetermined combination of data modulation and channel coding rate when performing AMC.

*17 **Symbol**: A unit of data for transmission. In OFDM, it comprises multiple subcarriers (see *21). A CP (see *36) is inserted at the head of each symbol.

*18 **CDM**: When transmitting multiple signal sequences on the same radio system band, mul-

tiplexing them using spreading sequences.

*19 **Channel estimation**: The process of estimating the amount of fluctuation in received attenuation and phase rotation in the received signal when a signal is transmitted over a radio channel.

*20 **CSI**: Information describing the state of the radio channel traversed by the received signal.

RS is multiplexed at the 11th symbol of the sub-frame; this RS is transmitted periodically at intervals corresponding to a T_{CSI} sub-frame (time unit for providing CSI feedback and updating precoding weights). In addition, CSI-RS for each transmitter antenna is multiplexed using Frequency Division Multiplexing (FDM)^{*22}, which is mapped every six subcarriers. Meanwhile, DM-RS, which is precoded in the same manner as the data streams, is mapped at a density of 12 Resource Elements (REs) per transmission stream within one RB in each sub-frame. In the case of Rank-4 MU-MIMO, DM-RS between the two streams for the same MS applies CDM while DM-RS between different MSs applies FDM as shown in the figure.

In this experimental equipment, the MS calculates eigenvalues and eigenvectors, which are obtained by performing eigenvalue decomposition against the covariance matrix^{*23} of the MIMO channel matrix^{*24} estimated using CSI-RS, and received Signal-to-Interference plus Noise power Ratio (SINR)^{*25} as CSI feedback. In each sub-band, quantization^{*26} is applied to an eigenvector up to a maximum of 13 bits (amplitude: 6 bits; phase: 7 bits) using Star-type mapping for each transmitter antenna of each stream. It is also applied to an eigenvalue and received SINR at 5 and 7 bits, respectively, for each stream. The BS uses this CSI feedback from the

2 MSs to calculate precoding weights based on Minimum Mean Square Error (MMSE) criterion^{*27} in each sub-band and multiplies the corresponding data streams by those weights before transmission.

2.4 Downlink CoMP Transmission

For this experimental equipment, we have implemented a function for testing CoMP Multi-User Joint Trans-

mission (MU-JT)^{*28} by using BS transmitter antennas which are located at multiple points, i.e., RRE, for the downlink MU-MIMO described above (Figure 6). We plan to perform experimental evaluations in laboratory and field environments in the future.

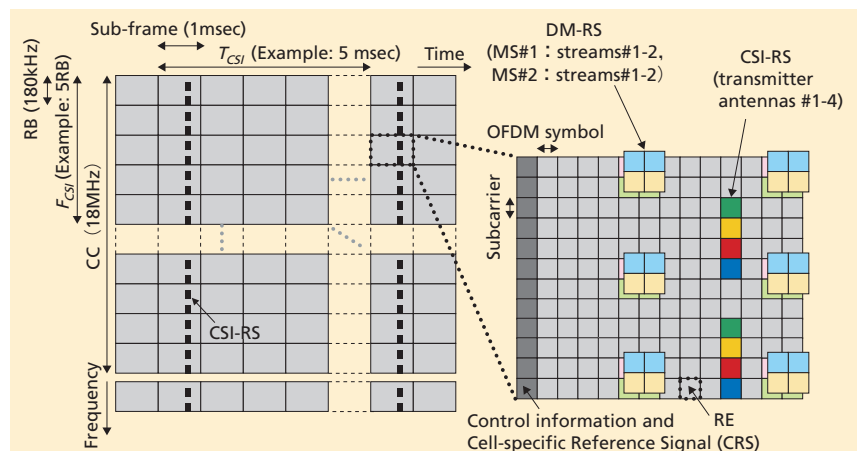


Figure 5 Downlink sub-frame configuration in experimental equipment

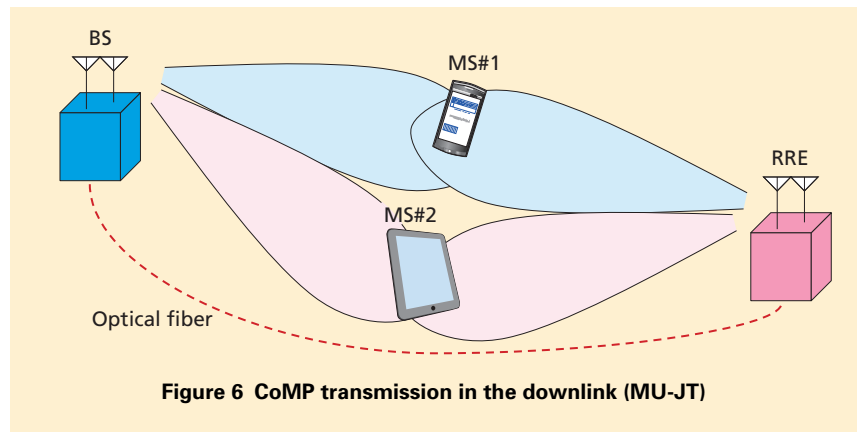


Figure 6 CoMP transmission in the downlink (MU-JT)

*21 **Subcarrier:** One of the individual carrier waves used to transmit a signal in multi-carrier transmission schemes such as OFDM.
 *22 **FDM:** When transmitting multiple signal sequences on the same radio system band, multiplexing them using frequencies that are mutually orthogonal.
 *23 **Covariance matrix:** A matrix whose diagonal components express the variance of each variable in a set of variables and whose other

elements each express the degree of correlation between two variables with respect to their direction of change (positive/negative).
 *24 **Channel matrix:** A matrix composed of the changes in amplitude and phase on the radio channels among transmitter and receiver antennas.
 *25 **Received SINR:** The ratio of desired-signal power to the total power from interference from other users in the same cell, interference

from other cells and sectors, and from noise within the received signal.
 *26 **Quantization:** In digital communications, approximation of the amplitude and phase of an analog signal using discrete digital values.
 *27 **MMSE criterion:** A method for determining a signal that minimizes the mean square error.

3. Configuration of LTE-Advanced Transceiver

Basic specifications of the LTE-Advanced experimental equipment are shown in **Table 1** and the BS/MS transmitter/receiver configuration is shown in **Figure 7**.

3.1 Transmitter/receiver Configuration in the Downlink

In the downlink using OFDMA radio access, we employ CA using 5 CCs (each CC has an 18 MHz transmission bandwidth). System bandwidth is 100 MHz (occupied signal bandwidth: 90 MHz) and the number of subcarriers is 6,000 (thus, subcarrier separation is 15 kHz).

The transmitter/receiver configuration in the downlink is shown in Fig. 7(a). The BS transmitter first applies turbo coding^{*29} using channel coding rate^{*30} R with a constraint length^{*31} of four bits to the information binary bit sequence, and then performs data modulation using Quadrature Phase Shift Keying (QPSK)^{*32}, 16Quadrature Amplitude Modulation (QAM)^{*33} or 64QAM^{*34}. Next, the transmitter multiplexes DM-RS on the data-modulated sequence, multiplies the precoding weight calculated using the CSI feedback from each MS with the corresponding data stream and DM-RS, and

generates signals for four transmitter antennas. In this evaluation, the sub-band size of CSI feedback is set to $F_{CSI} = 5$ RB (900 kHz) and CSI-RS transmission period (CSI feedback period) is set to $T_{CSI} = 5$ msec. For each transmitter antenna, the transmitter converts the data sequence multiplexed with CSI-RS to a time domain signal by an Inverse Fast Fourier Transform (IFFT)^{*35} with 8,192 points and inserts a Cyclic Prefix (CP)^{*36} at the head of each symbol. Finally, the transmitter performs D/A conversion and quadrature modulation on the OFDMA signal so generated and transmits the signal after up-converting it a 3.92625 GHz carrier frequency.

The MS receiver, applies 2-branch antenna-diversity reception. The receiver

first down-converts the received signal of each branch to an intermediate frequency. It then linearly amplifies the signal by an Automatic Gain Control (AGC)^{*37} amplifier having a dynamic range of approximately 50 dB. The receiver next converts the signal into in-phase and quadrature-phase components by a quadrature detector and converts them into a digital format using 14-bit A/D conversion. It then deletes CP from the received digital signal, converts the signal to a frequency domain signal by a Fast Fourier Transform (FFT)^{*38}, calculates a channel estimation value^{*39} using the received DM-RS, and performs coherent detection on the data signal. After an interference whitening filter is applied in order to

Table 1 Basic specifications of experimental equipment

| | Downlink | Uplink |
|---|---|-----------------|
| Radio access | OFDMA | SC-FDMA |
| Carrier frequency | 3.92625 GHz | 3.67125 GHz |
| System bandwidth | 100 MHz | 40 MHz |
| Transmission power | Field: 10 W (40 dBm) Indoor: 100 mW (20 dBm) | 200 mW (23 dBm) |
| Number of transmitter/receiver antennas | BS : 4 / MS : 2 | |
| Number of CCs | 5 | 2 |
| Number of subcarriers | 6,000 | 2,400 |
| Subcarrier separation | 15 kHz | |
| Sub-frame length | 1 msec | |
| Symbol length | 66.67 μsec + CP 4.69 μsec | |
| Data modulation | QPSK, 16QAM, 64QAM | |
| Channel encoding/decoding | Turbo encoding ($R = 0.38 - 0.92$) / Max-Log-MAP decoding | |
| MIMO signal detection | MLD | MMSE |

*28 **CoMP MU-JT**: A technology that improves spectral efficiency by simultaneously transmitting signals to multiple users from multiple sectors or cells and performing MIMO multiplexed transmission.

*29 **Turbo coding**: A kind of error correction coding. The reliability information in the decoded results can be used for iterative decoding to obtain powerful error correction capabilities.

*30 **Channel coding rate**: The ratio of the number of data bits to the number of bits after error correction coding.

*31 **Constraint length**: Represents the number of past input bits required to obtain the output. In general, a large constraint length means a high error correction capability.

*32 **QPSK**: A digital modulation method that uses a combination of signals with four different phases to enable the simultaneous transmission of two bits of data.

*33 **16QAM**: A digital modulation method that allows transmission of 4 bits of information simultaneously by assigning one value to each of 16 different combinations of amplitude and phase.

*34 **64QAM**: A digital modulation method that allows for transmission of 6 bits of information simultaneously by assigning one value to each of 64 different combinations of amplitude and phase.

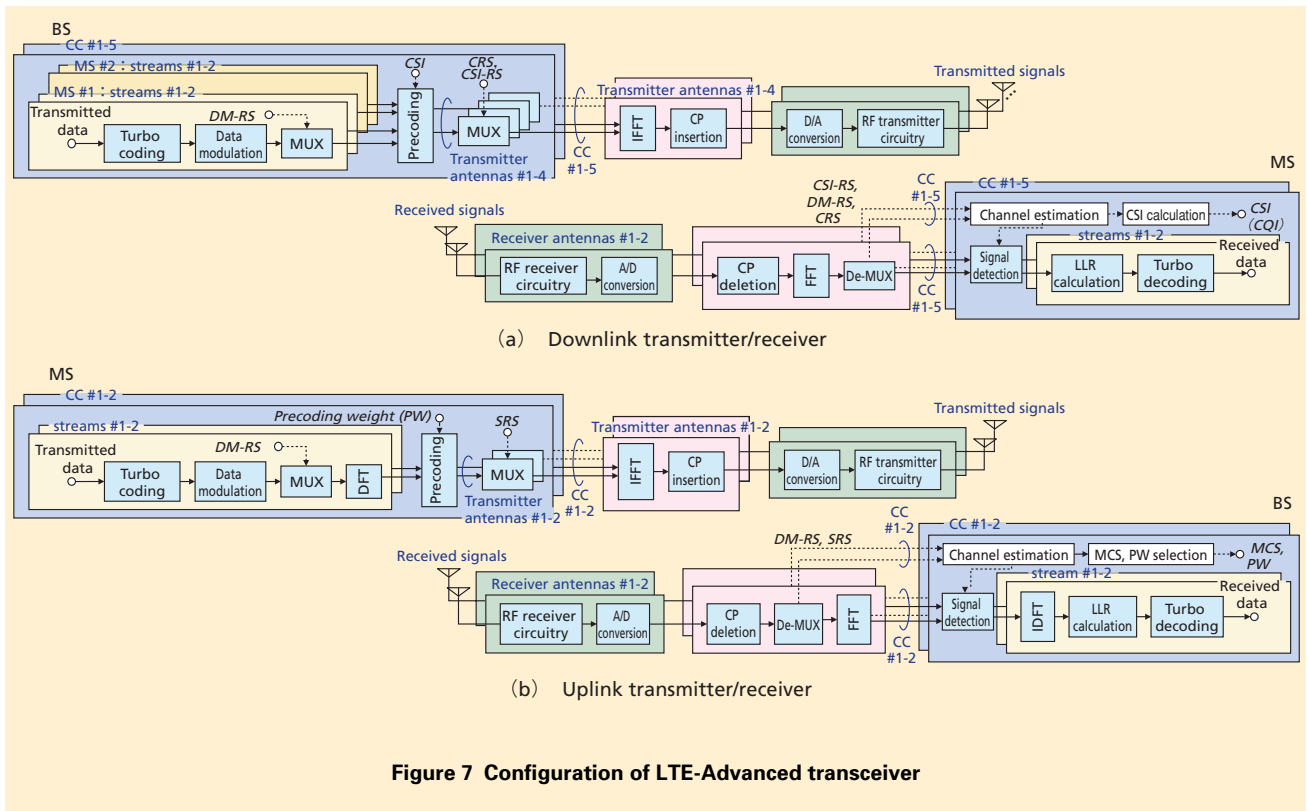


Figure 7 Configuration of LTE-Advanced transceiver

randomize the interfering data streams that are transmitted to the other MS, the Maximum Likelihood Detection (MLD)^{*40} is performed to separate the two data streams that are transmitted to its own MS. After signal detection, the receiver takes the signal and calculates the Log Likelihood Ratio (LLR) for each bit for the purposes of soft-decision turbo decoding, performs turbo decoding by the Max-Log-MAP^{*41} algorithm, and recovers the transmitted signal sequence. The MS also calculates CSI using the received CSI-RS and feeds it back to the BS.

3.2 Transmitter/receiver Configuration in the Uplink

In the uplink based on SC-FDMA using Discrete Fourier Transform (DFT)-Spread OFDM^{*42} [19], we employ CA using 2 CCs (each CC has an 18-MHz transmission bandwidth). System bandwidth is 40 MHz (occupied signal bandwidth: 36 MHz) and the number of subcarriers is 2,400 (thus, subcarrier separation is 15 kHz).

The transmitter/receiver configuration in the uplink is shown in Fig. 7(b). The MS transmitter first performs turbo coding using channel coding rate R with a constraint length of four bits on

the information binary bit sequence, and then performs data modulation using QPSK, 16QAM or 64QAM. The transmitter then converts the modulated data sequence into a frequency domain signal by DFT, and in the case of rank 1, multiplies the precoding weight reported from the BS with the corresponding data stream and DM-RS, and generates signals for two transmitter antennas. Here, DM-RS and SRS are multiplexed with their corresponding symbols in the manner shown in Fig.3. In this evaluation, the SRS transmission period is set to $T_{SRS} = 5$ msec. Finally, the transmitter converts each of the

*35 IFFT: A method for efficiently computing the time signal series corresponding to input frequency components (discrete data).

*36 CP: A guard time inserted between symbols in OFDM signals, etc. to minimize interference between prior and subsequent symbols caused by multipath effects.

*37 AGC: A function for automatically adjusting amplification in a receiver's power amplifier so that the amplitude of the output signal is

constant.

*38 FFT: A high-speed computation method for extracting the frequency components of a time domain signal.

*39 Channel estimation value: The estimated amount of fluctuation in received attenuation and phase rotation when a signal traverses a radio channel, computed using a reference signal multiplexed on the packet frame.

*40 MLD: A method for separating MIMO multi-

plexed signals by comparing all sequences of received signals with those that could possibly be received and finding the combination nearest the received pattern.

transmitter antenna signals to a time domain signal by IFFT with 4,096 points, inserts CP at the head of each symbol, performs D/A conversion and quadrature modulation on the SC-FDMA signal so generated, and transmits the signal after up-converting it to a 3.67125 GHz carrier frequency.

The BS receiver applies 2-branch antenna-diversity reception. For each branch, the receiver performs linear amplification by an AGC amplifier and quadrature detection on the received signal followed by A/D conversion. It then deletes CP from the receive digital signal, obtains a data signal separated by FFT into frequency signal components, and subjects this data signal to frequency domain equalization based on MMSE criterion in the case of rank 1 and to signal detection between the transmission streams in MIMO spatial multiplexing in the case of rank 2. Channel estimation and noise power estimation used for equalization and signal detection here are calculated using the DM-RS received for each stream. Finally, the receiver converts the equalized signal to a time domain signal by Inverse DFT (IDFT)^{*43}, calculates LLR for each bit of that signal for the purposes of soft-decision turbo decoding, and recovers the transmitted signal sequence by turbo decoding. The BS receiver also determines the MCS and precoding weight using the

received SRS and notifies the MS thereof.

4. Field Experiments for CA and 2 × 2 SU-MIMO

4.1 Measurement Courses for Field Experiment

The field experiment was performed in two areas: the Yokosuka Research Park (YRP) district in Yokosuka City (Figure 8 (a)) and the downtown district of Sagamihara City (Fig. 8 (b)), both in Kanagawa Prefecture, Japan. Two measurement courses were used in the YRP district: course #1 in a Line-Of-Sight (LOS) environment with a distance from the BS of 120 - 350 m and course #2 in a Non-Line-Of-Sight (NLOS) environment with a distance from the BS of 350 - 470 m. The height of the BS antenna was 39.6 m. Course #3 in downtown Sagamihara City, meanwhile, passed through a mixture of LOS and NLOS environments in an

area dominated by office buildings and high-rise condominium buildings. Distance from the BS was 400 - 820 m and the height of the BS antenna was 56.6 m. Each BS antenna had a 3 dB beam width of approximately 90 degrees in azimuth and used a 2-branch transmitter/receiver antenna with an antenna gain of approximately 18 dBi. The total transmission power was set to 10 W (40 dBm).

In this field experiment, the MS antenna was installed on the ceiling of a measurement vehicle at a height of 3.1 m. It consisted of a 2-branch transmitter/receiver antenna omni-directional in azimuth. The total transmission power was set to 200 mW (23 dBm). The measurement vehicle loading the MS equipment travelled along each of the above measurement courses at a speed of approximately 10 or 30 kilometers per hour (km/h). Two vertically polarized antennas set at a certain distance

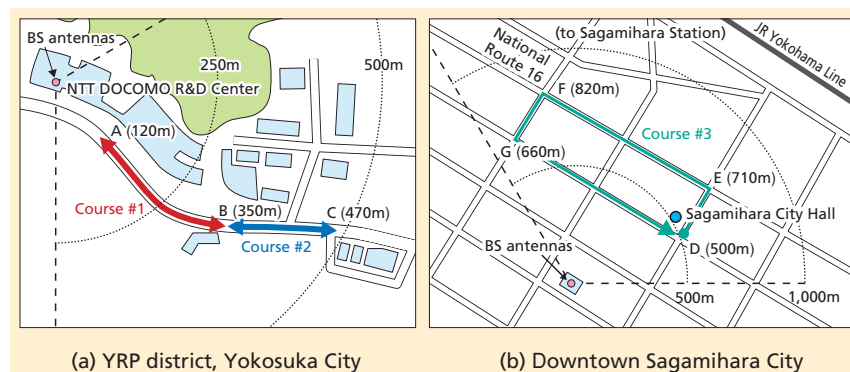


Figure 8 Measurement courses in field experiment

*41 **Max-Log-MAP**: A channel-decoding algorithm that can achieve nearly equivalent characteristics of Maximum A posteriori Probability (MAP), an optimal decoding algorithm, while significantly reducing computational complexity by using approximations in computing a posteriori probability.

*42 **DFT-Spread OFDM**: A method for generating SC-FDMA signals in the frequency domain using DFT processing. Signal processing after

DFT has much in common with OFDM.

*43 **IDFT**: The inverse of a discrete Fourier transform converting discrete data in the frequency domain to discrete data in the time domain.

from each other were used for both the BS and MS in all cases other than the evaluation of Figure 13. That evaluation in Figure 13 used cross-polarized antennas consisting of a vertically polarized antenna and horizontally polarized antenna housed in one rack.

Figure 9 shows examples of the measured power delay profile^{*44} in the downlink of each measurement course. The vertical axis represents received power normalized with respect to a noise power level measured in the region for which no signal paths exist. From these results, in course #1, we clearly observed two dominant paths with high signal received level, one of a direct wave and the other of a reflected wave. In course #2, on the other hand, many distributed paths are distributed over approximately 1 μsec, while in course #3, larger delayed paths over 2-3 μsec are observed compared to course #2.

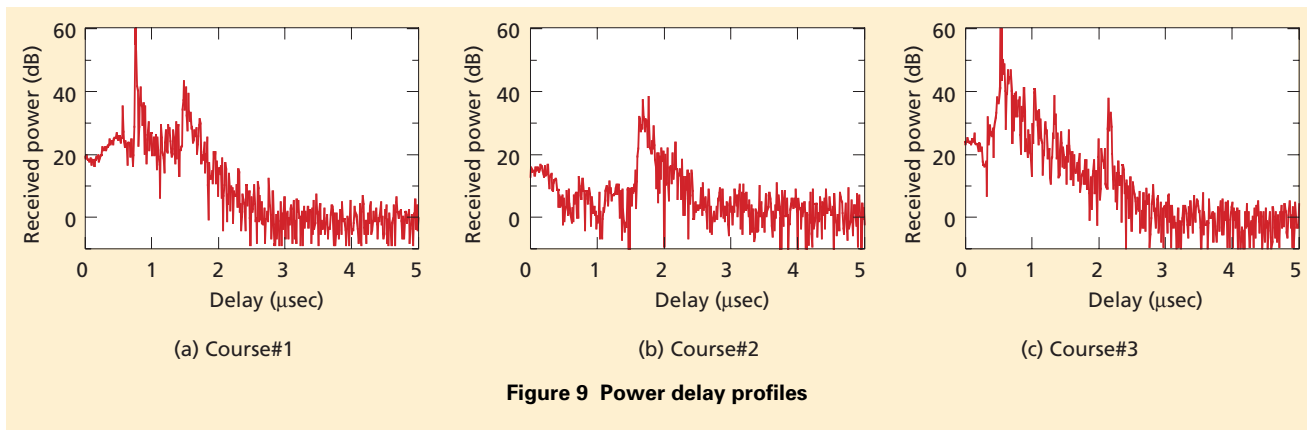
4.2 Field Experimental Results

In evaluating 2 × 2 Rank-2 SU-MIMO in the downlink, we applied MIMO spatial multiplexing (with no precoding) in which an independently encoded stream is transmitted from each of two antennas, the same as in 2 × 2 Rank-2 SU-MIMO in the uplink.

Figure 10 shows examples of time variation of the measured average received SINR over 5 CCs, the MCS selection probability, and the measured total throughput over 5 CCs at the MS, when applying CA with 5 CCs and 2 × 2 Rank-2 SU-MIMO in courses #1 and #2 (YRP district). In these measurements, we had the MS move at a speed of 10 km/h and applied AMC and HARQ. The received SINR and throughput are averaged over a duration of 100 msec and the MCS selection probability is measured in 1-sec intervals. First, the figure shows that the received SINR values in excess of 20 dB could be observed on course #1

thanks to the LOS environment. On course #2, however, the received SINR degrades as the distance from the BS antenna increases and consequently becomes almost 0 dB in the vicinity of point C (470 m) where the course terminated. In short, for course #1, a high-data-rate MCS using 64QAM was selected with a high probability that throughput would be greater than 500 Mbit/s for the majority of the course. On course #2, in contrast, the appropriate MCS was adaptively selected according to the measured received SINR value, and at the course termination point, a throughput of only 50-100 Mbit/s could be observed.

Figure 11 shows the Cumulative Distribution Function (CDF)^{*45} of measured throughput averaged over a duration of 100 msec for each measurement course when applying CA with 5 CCs and 2 × 2 Rank-2 SU-MIMO in the downlink. For course #1, while throughput at a MS-speed of 30 km/h



*44 **Power delay profile:** A plot representing the delay time of paths arriving at the receive point on the horizontal axis and their received power on the vertical axis.

*45 **CDF:** A distribution of a stochastic variable in a cumulative form.

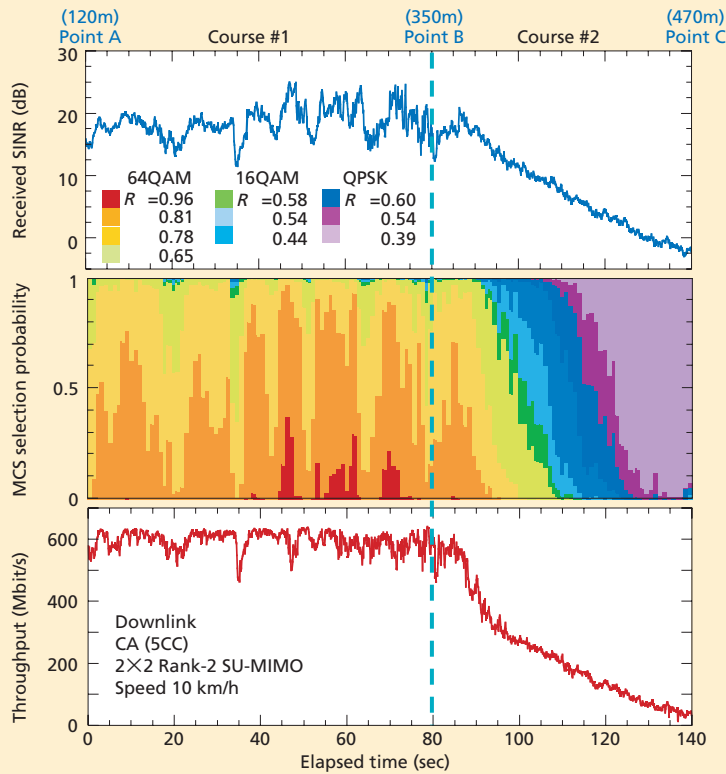


Figure 10 Time variation of received SINR, MCS selection probability, and throughput in the downlink

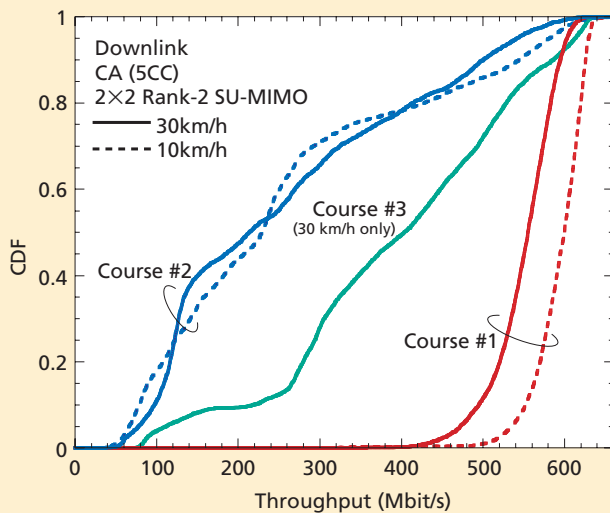


Figure 11 Throughput performance of CA and SU-MIMO in the downlink

was inferior to that at 10 km/h due to less accurate channel estimation, a throughput performance greater than 500 Mbit/s was achieved at a location probability of approximately 90% on the course. For course #2, although larger MCS selection error occurred at 30 km/h compared to 10 km/h due to the decrease in tracking ability with respect to AMC operation for the instantaneous fading variation, the achievable throughput at a MS-speed of 30 km/h was almost the same as that at 10 km/h. The reason for this is considered to be that, thanks to HARQ operation, the decrease in throughput performance was suppressed to a minimum level. Finally, for course #3 (the multipath environment in downtown Sagami-hara City), throughput was better than that of course #2 despite the fact that distance from the BS antenna was greater than that of the measurement courses in the YRP district. As a result, a throughput performance greater than 500 Mbit/s was achieved at a location probability of approximately 30% on the course. One of the reasons for this is considered to be that the BS antenna height in downtown Sagami-hara City is higher than that in the YRP district.

We next present throughput performance for SU-MIMO transmission in the uplink. **Figure 12** shows CDF of measured throughput averaged over a

duration of 100 msec for the entire measurement course in the YRP district (combining courses #1 and #2) when applying CA with 2 CCs and 2 × 2 Rank-2 and Rank-1 SU-MIMO. Here, we applied AMC and HARQ and had the MS move at a speed of 10 km/h. For comparison, we also plotted the performance for 1 × 2 Single-Input Multiple-Output (SIMO)^{*46}. This figure shows that throughput in the case of rank 1 was superior to that of 1 × 2 SIMO for nearly the entire course (in particular, the throughput increased by approximately 50% at 20% of the CDF). This result demonstrates the coverage expansion effect of closed-loop transmission diversity. In the case of rank 2, moreover, the throughput performance greater than 140 Mbit/s (a peak throughput of approximately 200 Mbit/s) was achieved at a location probability of approximately 25% on the course. This result demonstrates the effectiveness of throughput enhancement of MIMO spatial multiplexing in the uplink in a field environment.

Figure 13 shows CDF of measured throughput averaged over a duration of 100 msec for course #3 in downtown Sagami-hara City when applying CA with 2 CCs and 2 × 2 Rank-2 and Rank-1 SU-MIMO. For this evaluation, we used cross-polarized antennas for MS and BS, applied AMC and HARQ, and set the speed of the MS to 30 km/h.

For comparison, we also plotted the performance for co-polarized (vertically polarized) antennas (it should be noted that the results for co-polarized anten-

nas indicate those when high received power is obtained because all polarization planes are the identical). First, examining the results for rank 2, it can

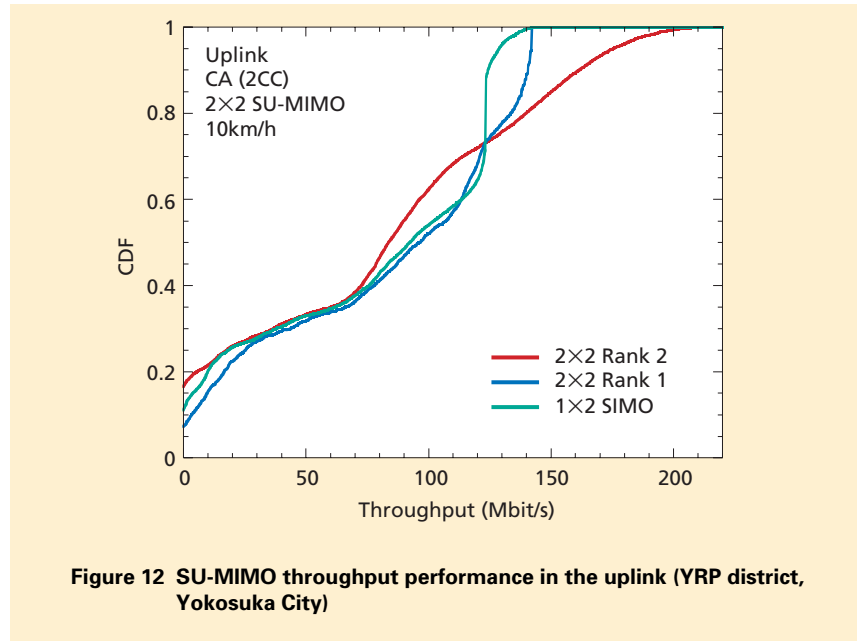


Figure 12 SU-MIMO throughput performance in the uplink (YRP district, Yokosuka City)

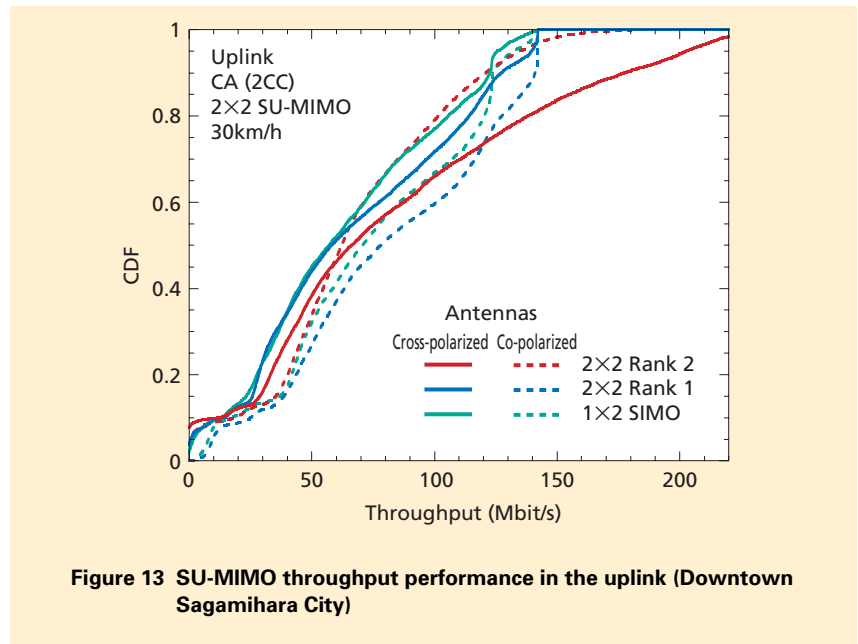


Figure 13 SU-MIMO throughput performance in the uplink (Downtown Sagami-hara City)

^{*46} **SIMO**: A signal-transmission method that, compared to MIMO, uses only one transmitter antenna and multiple receiver antennas.

be seen that for the co-polarized antennas, the location probability that rank 2 is effective in improving the throughput was only approximately 3% and a peak throughput of only approximately 170 Mbit/s was achieved due to severe multipath interference. These results differ from those obtained in the YRP district (Fig. 12). When using cross-polarized antennas, however, the location probability that rank 2 is effective in improving the throughput was greatly improved and a peak throughput of approximately 230 Mbit/s was achieved. This is because, while overall received power (receive diversity gain) decreased in this case since the received signal power received at different polarization planes was relatively smaller, inter-stream interference in MIMO spatial multiplexing could be significantly decreased overcoming the above disad-

vantage. In the case of rank 1, throughput performance was greatly improved at a location probability of approximately 45% on the course compared to 1×2 SIMO.

5. Indoor Experiments for 4×2 MU-MIMO in the Downlink

5.1 Measurement Environment and Evaluation Conditions

We investigated the measured throughput in a conference room at the NTT DOCOMO R&D Center. A photograph showing the experimental layout in the conference room is shown in **Figure 14**. The room was 18.4 m wide, 12.2 m deep, and 3.8 m high, and 40 desks and 80 chairs were set up. The BS antennas were located at the center of the room, and measurements were performed while keeping MS#1 station-

ary near point P on the experimental course and moving MS#2 from point P to point Q at a speed of 1 km/h. The total length of the course was approximately 14 m. The heights of the BS and MS antennas were 2.4 and 1.4 m, respectively, and both the BS and MS used dipole antennas omni-directional in azimuth with an antenna gain of approximately 2 dBi. Adjacent antennas were arranged in a linear manner at an interval of 7.6 cm (corresponding to one wavelength of the downlink carrier frequency) and BS transmission power was set to 100 mW (20 dBm). Over the entire course, the BS antennas were in direct view from the MS antennas, i.e., LOS conditions. The root mean squared (r.m.s.) delay spread^{*47} of the measurement course, which is calculated based on the received CSI-RSSs, was approximately 0.05 μ sec, and the fading correlation^{*48} between adjacent transmitter antennas and that between adjacent receiver antennas were 0.42 and 0.30, respectively.

In this evaluation, we measured throughput performance using AMC and HARQ when 4×2 MU-MIMO using 2 MSs in the downlink and CA with 5 CCs (100-MHz bandwidth) were applied. The AMC is performed based on the instantaneous received SINR reported by the MS. However, the received SINR in the case of MU-MIMO varies greatly owing to mutual

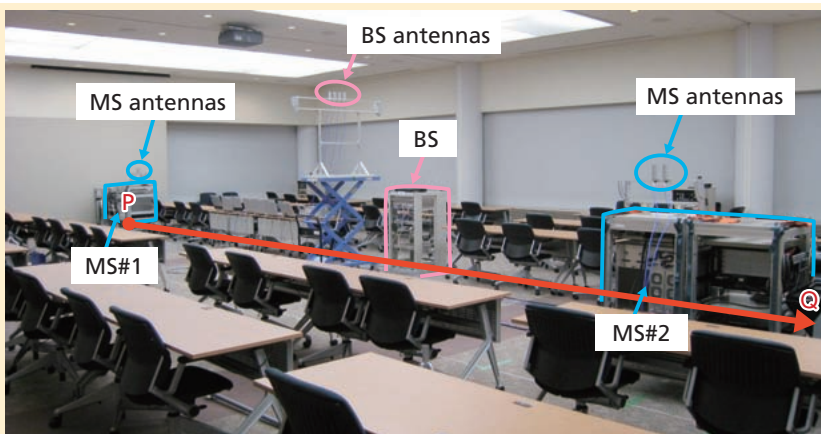


Figure 14 Measurement course in indoor experiment (conference room at NTT DOCOMO R&D Center)

^{*47} **r.m.s. delay spread:** In signal propagation in mobile communications, the delay-time spread of all radio waves arriving late owing to reflection and diffraction off of buildings and other structures. The delay time of all arriving waves is defined by a standard deviation computed by weighted statistical processing using received power.

^{*48} **Fading correlation:** In this article, an index indicating the correlation of fading between different antennas used in MIMO transmission.

interference between MSs, which can increase MCS selection error. To therefore reduce the error in this experimental equipment, we implemented outer-loop threshold control^{*49} [20] to adaptively adjust MCS selection thresholds based on ACK/NACK feedback signaling from the MS.

5.2 Indoor Experimental Results

To begin with, we explain the basic performance of 4×2 Rank-4 MU-MIMO in a laboratory experiment using a fading simulator. In this evaluation, we assumed a correlated BS antenna scenario using two high-correlated transmitter antenna pairs (in which the fading correlation between the two pairs was set to 0.99, that between the two transmitter antennas in a pair was set to 0.0, maximum Doppler frequency was set to 10 Hz (corresponding to a MS speed of approximately 3 km/h), and a 6-path exponentially decayed channel model with a r.m.s. delay spread of 0.3 μ sec was assumed). **Figure 15** shows total throughput performance for MU-MIMO, which is defined as the aggregated throughput for each MS, as a function of the average received Signal-to-Noise power Ratio (SNR)^{*50}. The throughput performance for the respective MCS combination is also given for comparison. This figure shows that by employing the MCS combination of 64QAM, $R =$

0.73 for stream #1 and 64QAM, $R = 0.56$ for stream #2, a peak throughput of approximately 1 Gbit/s was achieved. Furthermore, we clearly find that applying AMC results in nearly the maximum throughput at each average received SNR, since the appropriate MCS is selected based on the instantaneous measured SINR. As a result, we observed that a peak throughput of approximately 1 Gbit/s was achieved.

Next, **Figure 16** shows examples of the time variation of measured throughput for each MS and 2-MS total when applying 4×2 Rank-4 MU-MIMO in the indoor environment shown in Fig. 14 (conference room). Here, the throughput was averaged over a duration of 200 msec. This figure shows that the throughput of not only the moving MS (MS#2) but also of the

stationary MS (MS#1) varies with elapsed time. The reason for this is considered to be that the propagation environment surrounding MS#1 is also fluctuating owing to the movement of MS#2 resulting in the updating of precoding weights. This figure also shows that by applying 4×2 Rank-4 MU-MIMO using CSI feedback based on eigenvalue decomposition, a peak throughput of approximately 1 Gbit/s is achieved. Furthermore, considering the fact that the achievable throughput for 4×2 SU-MIMO is 600 - 700 Mbit/s over the entire measurement course, we confirm the superiority of MU-MIMO compared to SU-MIMO in an indoor environment.

6. Conclusion

In this article, we described experi-

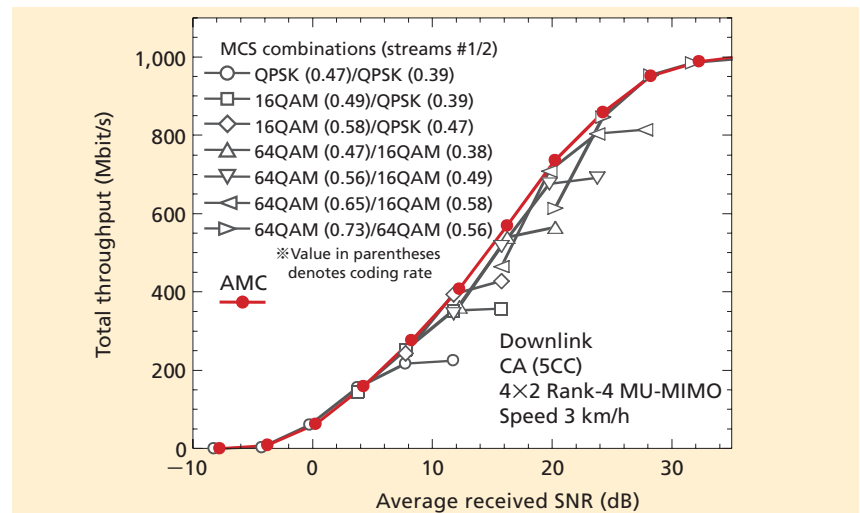


Figure 15 Throughput performance of 4×2 MU-MIMO in the downlink (laboratory experiment)

*49 **Outer-loop threshold control:** In this article, a method for adaptively controlling the MCS selection threshold according to received quality of data for selecting MCS in AMC.

*50 **Received SNR:** Ratio of desired signal power to noise power in the received signal.

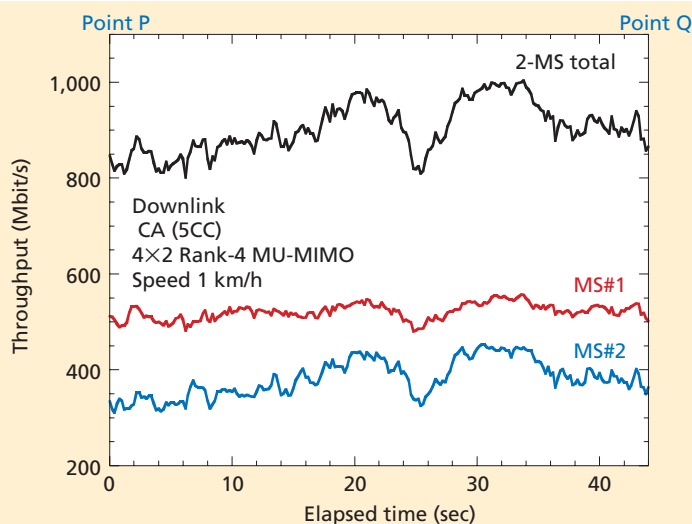


Figure 16 Time variation of 4×2 MU-MIMO throughput in the downlink

mental equipment for testing LTE-Advanced radio access technology based on LTE Release 10 specifications. This equipment implements CA (to achieve wider transmission bandwidths up to 100 MHz in the downlink and 40 MHz in the uplink) as a basic function. It enables evaluation experiments to be performed on the use of advanced multi-antenna technologies in LTE-Advanced such as SU-MIMO transmission in the uplink and MU-MIMO/CoMP transmission in the downlink. We also presented and discussed the results of transmission experiments using this experimental equipment in field and indoor propagation environments. First, in the field experiment, we showed that a peak throughput greater than 600 Mbit/s in the downlink and 200 Mbit/s in the

uplink could be achieved by applying CA and 2×2 Rank-2 SU-MIMO. Then, in the indoor experiment, we showed that a peak throughput of approximately 1 Gbit/s could be achieved in the downlink by applying 4×2 Rank-4 MU-MIMO using 2 MSs and CA (100-MHz bandwidth).

Looking forward, we plan to continue evaluation experiments on MU-MIMO/CoMP downlink transmission technology in laboratory and field environments.

REFERENCES

[1] 3GPP TS36.300 V8.12.0: “Evolved Universal Terrestrial Radio Access (EUTRA) and Evolved Universal Terrestrial Radio Access Network (E-UTRAN); Overall description; Stage 2,” Apr. 2010.
 [2] N. Okubo et al.: “Overview of LTE Radio Interface and Radio Network Architecture

for High Speed, High Capacity and Low Latency,” NTT DOCOMO Technical Journal, Vol. 13, No. 1, pp. 10-19, Jun. 2011.

[3] T. Nakamura et al.: “Overview of LTE-Advanced and Standardization Trends,” NTT DOCOMO Technical Journal, Vol. 12, No. 2, pp. 4-9, Sep. 2010.
 [4] S. Nagata, D. Nishikawa, T. Abe, Y. Kishiyama and T. Nakamura, “System Performance Evaluation for LTE/LTE-Advanced,” IEICE Technical Report, Vol. 110, No. 19, RCS2010-5, pp. 25-30, Apr. 2010 (In Japanese).
 [5] M. Iwamura, K. Etemad, M. Fong, R. Nory and R. Love: “Carrier Aggregation Framework in 3GPP LTE-Advanced,” IEEE Trans. Commun. Mag., Vol. 48, No. 8, pp. 60-67, Aug. 2010.
 [6] 3GPP TS36.201 V10.0.0: “Evolved Universal Terrestrial Radio Access (EUTRA); LTE physical layer; General description,” Dec. 2010.
 [7] E. Dahlman, S. Parkvall and J. Sköld: “4G-LTE/LTE-Advanced for Mobile Broadband,” Academic Press, 2011.
 [8] Y. Kakishima, T. Kawamura, Y. Kishiyama, H. Taoka and T. Nakamura: “Experimental Evaluation on Throughput Performance of Asymmetric Carrier Aggregation in LTE-Advanced,” Proc. of IEEE VTC2011-Spring, May 2011.
 [9] S. Yasukawa, T. Kawamura, Y. Kishiyama, H. Taoka and T. Nakamura: “Experimental Evaluation on SU-MIMO Transmission with Closed-Loop Precoding in LTE-Advanced Uplink,” Proc. of IEEE VTC2011-Spring, May 2011.
 [10] S. Yasukawa, T. Kawamura, Y. Kishiyama, H. Taoka and T. Nakamura: “Experiments on Throughput and Coverage for Closed-Loop SU-MIMO Transmission Combined with Carrier Aggregation in LTE-Advanced Uplink,” Proc. of IEEE APWCS, Aug. 2011.

- [11] Y. Kakishima, K. Takeda, T. Kawamura, Y. Kishiyama, H. Taoka and T. Nakamura: “Experimental Evaluations on Carrier Aggregation and Multi-user MIMO Associated with EVD-based CSI Feedback for LTE-Advanced Downlink,” Proc. of IEEE ISWCS, Nov. 2011.
- [12] K. Saito, Y. Kakishima, T. Kawamura, Y. Kishiyama, H. Taoka and H. Andoh: “Experimental Evaluation on 4-by-2 MUMIMO Achieving 1 Gbps Throughput Using AMC with Outer-Loop Threshold Control for LTE-Advanced Downlink,” Proc. of IEEE VTC2012-Spring, May 2012.
- [13] S. Yasukawa, T. Kawamura, Y. Kishiyama, H. Taoka and H. Andoh: “Field Experiments on Closed-Loop SU-MIMO Transmission Considering Effect of Antenna Configurations in LTE Advanced Uplink,” Proc. of IEEE VTC2012-Spring, May 2012.
- [14] Y. Kakishima, T. Kawamura, Y. Kishiyama, H. Taoka and H. Andoh: “Experiments on Downlink 4-by-2 MU-MIMO with Quantized CSI Feedback for LTE-Advanced Deployment Scenarios,” Proc. of Future Network and Mobile Summit, Jul. 2012.
- [15] K. Saito, Y. Kakishima, T. Kawamura, Y. Kishiyama, H. Taoka and H. Andoh: “Field Experiments on Throughput Performance of Carrier Aggregation with Asymmetric Bandwidth in LTE-Advanced,” Proc. of Future Network and Mobile Summit, Jul. 2012.
- [16] M. Tanno, Y. Kishiyama, H. Taoka, N. Miki, K. Higuchi and M. Sawahashi: “Requirements and Technologies for LTE-Advanced Radio Access,” IEICE Technical Report, Vol. 108, No. 305 RCS2008-136, pp. 37-42, Nov. 2008 (In Japanese).
- [17] M. Tanno, Y. Kishiyama, H. Taoka, N. Miki, K. Higuchi and M. Sawahashi: “Layered OFDMA Radio Access for IMT-Advanced,” Proc. of IEEE VTC2008-Fall, Sep. 2008.
- [18] D. Tse and P. Viswanath: “Fundamentals of Wireless Communication,” Cambridge University Press, pp. 356-362, 2005.
- [19] D. Galda, H. Rohling, E. Costa, H. Haas and E. Schulz: “A Low Complexity Transmitter Structure for OFDM-FDMA Uplink Systems,” Proc. of IEEE VTC2002-Spring, pp. 1737-1741, May 2002.
- [20] J. Lee, R. Arnott, K. Hamabe and N. Takano: “Adaptive Modulation Switching Level Control in High Speed Downlink Packet Access Transmission,” 3G Mobile Communication Technologies, pp. 156-159, May 2002.